Biogeosciences

Photosynthetic responses of *Emiliania huxleyi* to UV radiation and elevated temperature: roles of calcified coccoliths

K. Xu[1], K. Gao[1], V. E. Villafañe[2], and E. W. Helbling[2]

[1]State Key Laboratory of Marine Environmental Science, Xiamen University, Xiamen, 361005, China
[2]Estación de Fotobiología Playa Unión and Consejo Nacional de Investigaciones Científicas y Técnicas (CONICET), Casilla de Correos No. 15, 9103 Rawson, Chubut, Argentina

Abstract. Changes in calcification of coccolithophores may affect their photosynthetic responses to both, ultraviolet radiation (UVR, 280–400 nm) and temperature. We operated semi-continuous cultures of *Emiliania huxleyi* (strain CS-369) at reduced (0.1 mM, LCa) and ambient (10 mM, HCa) Ca^{2+} concentrations and, after 148 generations, we exposed cells to six radiation treatments (>280, >295, >305, >320, >350 and >395 nm by using Schott filters) and two temperatures (20 and 25 °C) to examine photosynthesis and calcification responses. Overall, our study demonstrated that: (1) decreased calcification resulted in a down regulation of photoprotective mechanisms (i.e., as estimated via non-photochemical quenching, NPQ), pigments contents and photosynthetic carbon fixation; (2) calcification (*C*) and photosynthesis (*P*) (as well as their ratio) have different responses related to UVR with cells grown under the high Ca^{2+} concentration being more resistant to UVR than those grown under the low Ca^{2+} level; (3) elevated temperature increased photosynthesis and calcification of *E. huxleyi* grown at high Ca^{2+} concentrations whereas decreased both processes in low Ca^{2+} grown cells. Therefore, a decrease in calcification rates in *E. huxleyi* is expected to decrease photosynthesis rates, resulting in a negative feedback that further reduces calcification.

1 Introduction

Coccolithophores are organisms capable of fixing inorganic carbon into organic matter via photosynthesis as well as producing calcium carbonate crystals via intracellular calcifica-

tion. In addition to their role as primary producers, coccolithophores play a predominant function in global ocean calcification (Rost and Riebesell, 2004), accounting for up to half of the share (Milliman, 1993). While still is under debate, calcification in coccolithophores appears to be strongly linked to photosynthesis by favoring supply of CO_2 (Anning et al., 1996; Sikes et al., 1980; Sikes and Wilbur, 1982); moreover, Nimer et al. (1996) found reduced photosynthetic rates when removing external calcium. Other studies (Herfort et al., 2002, 2004; Trimborn et al., 2007; Leonardos et al., 2009) however, showed that changes in calcification under altered Ca^{2+} concentrations did not bring about concomitant changes in photosynthesis.

Calcification of coccolithophores is known to be influenced by many factors, such as light availability, nutrients, trace metals, CO_2 as well as temperature (Paasche, 2002; Shiraiwa, 2003; Zondervan, 2007) and ultraviolet radiation (UVR, 280–400 nm) (Gao et al., 2009; Guan and Gao, 2010). Under a scenario of global climate change, important changes in the physiology of diverse aquatic organisms are expected (Beardall et al., 2009; Häder et al., 2011), especially due to variations in UVR and temperature levels. In this sense, it has been found that UVR strongly influences photosynthesis and calcification of *Emiliania huxleyi* under CO_2-induced ocean acidification (Gao et al., 2009). In regard to the effects on coccolithophores of future ocean warming the results are rather varied: on the one hand, it was determined that photosynthesis could be promoted by increases in both pCO_2 and temperature (Feng et al., 2008) but, on the other hand, De Bodt et al. (2010) suggested that ocean acidification had a larger adverse impact than surface water warming on coccolithophorids' calcification.

Emiliania huxleyi (Lohmann) W. W. Hay and H. P. Mohler is a cosmopolitan species that frequently form blooms in shallow-mixed surface oceanic waters with high light exposures (Nanninga and Tyrrell, 1996). This species is therefore of key ecological importance and constitutes an excellent model to evaluate physiological responses under variable environmental stressors as those occurring due to global change. In particular, it has been found that growth and photosynthesis of *E. huxleyi* are highly affected by UVR (Buma et al., 2000; Guan and Gao, 2010); furthermore, enhanced acidification of seawater exacerbated detrimental UVR effects on photosynthesis (Gao et al., 2009). In the present study, we further investigated if variations in calcification rates in *E. huxleyi* altered its photosynthetic responses to both UVR and temperature, in a context of global change. The experimental approach was to incubate low- and high Ca^{2+} acclimated *E. huxleyi* cells to different radiation conditions (using an artificial source) and temperatures treatments (20 and 25 °C) to determine the energy-dependant responses (i.e., biological weighting functions, BWFs) of both photosynthesis and calcification.

2 Materials and methods

2.1 Organism and culture conditions

A coccolith-bearing strain of *Emiliania huxleyi* (CS-369) was obtained from the Commonwealth Scientific and Industrial Research Organisation (CSIRO, Australia). The cells were grown in artificial seawater enriched with 100 µM nitrate and 6.25 µM phosphate and with trace metals and vitamins as specified for the Aquil medium (Price et al., 1988/89). Two calcium concentrations were used in our experiments – adjusted to 0.1 mM (LCa) and 10 mM (HCa) by adding $CaCl_2$ – representing the reduced and ambient Ca^{2+} concentration of seawater, respectively. Ecologically, the reduced level of Ca^{2+} may be expected during coccolithophore blooms as observed in previous studies (Pitsyk, 1963; Cokacar et al., 2001; Mikaelyan et al., 2005) in estuarine systems where salinity was less than half the average oceanic value of ∼35. Physiologically, reduced Ca^{2+} availability is an effective way to investigate the role of calcification (Brownlee et al., 1995). Semi-continuous cultures were maintained at 20 °C at a PAR level of 150 µmol photons m^{-2} s^{-1} (12 L:12 D). The media (i.e., LCa and HCa) were renewed every 3 days, and cell concentrations were always kept $<10^5$ cells ml^{-1}. The cells were grown for at least 100 days (>148 generations) before being used in the experiments as described below.

2.2 Experimentation

Carbon incorporation and Pulse Amplitude Modulated (PAM) fluorescence measurements were done to assess the combined effects of ultraviolet radiation (UVR) and temperature on *Emiliania huxleyi*. Cells were exposed to

artificial radiation under a solar simulator (Sol 1200W; A. G. Hönle, Martinsried, Germany) at a distance of 120 cm from the lamp for 2 h. The irradiances output were measured with a broadband ELDONET filter radiometer (Real Time Computers, Möhrendorf, Germany) that has channels for PAR (400–700 nm), UV-A (315–400 nm) and UV-B (280–315 nm), and the measured values were 63.5 W m^{-2} (290 µmol photons m^{-2} s^{-1}), 23.1 W m^{-2} and 1.20 W m^{-2}, for PAR, UV-A and UV-B, respectively.

Biological weighting functions (BWFs) were used to separate the effects of different UV wavebands on photosynthesis, calcification, effective photochemical quantum yield of PSII (Y) and non-photochemical quenching (NPQ). Six different radiation treatments were set by using Schott cut-off filters that cut radiation below 280, 295, 305, 320, 350 and 395 nm (the transmission spectra of these filters are published elsewhere, Villafañe et al., 2003). For each experimental Ca^{2+} concentration, the samples were dispensed in six quartz tubes (14 ml) per radiation treatment (i.e., under each Schott filter). Thus a total of 36 tubes were irradiated; half of them were used for measurements of photosynthetic carbon fixation and calcification whereas the other half was used for PAM measurements (see below). The tubes containing the samples were put in a water bath for temperature control at 20 °C or 25 °C using a circulating cooler (CTP-3000, Eyela, Tokyo, Japan). Due to the effective irradiance area under the solar simulator, it was not possible to test the effects of both temperatures at the same time, so experiments were done one after the other. In this way we were sure that the irradiance received by the cells were the same.

2.3 Analyses and measurements

The pH was measured with a potentiometric titrator (DL15, Mettler-Toledo, Schwerzenbach, Switzerland) which was calibrated against Standard National Bureau of Standards (NBS) buffer solution (Hanna). The alkalinity of the media was also measured with the potentiometric titrator. The carbonate system was calculated from temperature, salinity, pH and concentrations of total alkalinity and phosphate, using the program CO_2sys (Lewis and Wallace, 1998). Equilibrium constants of Mehrbach et al. (1973) modified by Dickson and Millero (1987) were chosen for the calculations.

Just before experimentation, samples were taken for determination of pigments and quantification of cells. Cell densities were determined using a Coulter counter (Z2, Beckman Instruments, Florida, US) and specific growth rate was calculated as:

$$\mu = (\ln N_t - \ln N_0)/\Delta t$$

where N_0 and N_t are the cell concentrations after and before renewing the medium.

For pigments determination, 100 ml of sample was filtered onto Whatman GF/F filters (25 mm) under low pressure (200 mbar) and extracted overnight either in absolute

methanol (for chlorophyll-*a* (chl-*a*) determinations) or 90 % acetone (for carotenoids content) at 4 °C. After extraction and centrifugation (10 min at $5000 \times g$) the absorbance of the supernatant was determined with a scanning spectrophotometer (DU800, Beckman, Fullerton, California, USA). The chl-*a* content was calculated according to Porra (2002) whereas that of carotenoids using the equations of Strickland and Parsons (1972). In addition, an aliquot of 10 ml of culture (both from the HCa and LCa treatments) was filtered very gently onto 0.22 μm MCE (Mixed Cellulose Ester) filters (Xinya Instrument Co., Shanghai, China), washed three times with 0.2 M phosphate buffer (pH = 8) and then dried at 45 °C. The filters were coated with gold and then examined with a scanning electron microscope (Field Emission SEM, LEO 1530, Germany).

Fluorescence measurements were performed at 40, 80 and 120 min since the beginning of the incubations. Fluorescence parameters were determined with a pulse amplitude modulated fluorometer (model Xe-PAM, Walz, Effeltrich, Germany). The effective photochemical quantum yield of PSII (Y) was determined by measuring the instant maximal fluorescence (F'_m) and the steady state fluorescence (F_t) of light adapted cells using a saturating white light pulse (5000 μmol photons m^{-2} s^{-1} in 0.8 s) in the presence of a weak measuring light (0.3 μmol photons m^{-2} s^{-1}) and actinic light (300 μmol photons m^{-2} s^{-1}, i.e., similar PAR level as under the radiation treatments). Y was estimated according to Genty et al. (1989) as:

$$Y = (F'_m - F_t)/F'_m \tag{1}$$

UVR-induced inhibition of Y was calculated as:

$$\text{Inh (\%)} = (Y_{395} - Y_{320/280}) \cdot Y_{395}^{-1} \cdot 100 \tag{2}$$

where Y_{395} represents the Y under the PAR (395–700 nm) treatment, while $Y_{320/280}$ represents the Y under the PA (320–700 nm) or PAB (280–700 nm) treatments, respectively. Non-photochemical quenching (NPQ) was calculated as:

$$\text{NPQ} = (F_m - F'_m)/F'_m \tag{3}$$

where the F_m represents the maximum fluorescence yield after 10 min of dark adaptation.

For measurements of photosynthesis and calcification, samples (i.e., from the HCa and LCa treatments) were dispensed into 14 ml quartz tubes and inoculated with $100 \, \mu l - 10 \, \mu Ci$ (0.37 MBq) of NaH^{14}CO$_3$ (ICN Radiochemicals, Irvine, California, USA). After incubating for 2 h, subsamples for total (5 ml) and organic (5 ml) carbon were collected onto Whatman GF/F glass fiber filters (25 mm) under low pressure (200 mbar), rinsed three times with the medium and put in 20 ml scintillation vials. For the determination of organic carbon, the filters were exposed to HCl fumes overnight and dried at 45 °C; then they were digested in scintillation cocktail (Hisafe 3, Perkin-Elmer, Shelton, CT, USA)

and the activity of the fixed radiocarbon counted with a scintillation counter (Tri-Carb 2800TR, Perkin-Elmer, Shelton, CT, USA). The calcification rate was calculated as the difference between total (non acidified filters) and organic particulate carbon fixation (acidified filters) as previously reported (Gao et al., 2009; Guan and Gao, 2010).

Biological weighting functions (BWFs) for inhibition of Y, NPQ, photosynthetic carbon fixation and calcification were calculated using an exposure-response curve based on irradiance (Neale and Kieber, 2000). The biological responses for each wavelength interval over the incubation period were expressed as a function of the average irradiance (over incubation time) in the exposure wavelength interval. The relative spectral emission of the solar simulator was determined using a USB diode array spectroradiometer (HR 2000CG-UV-NIR, Ocean Optics, Duneclin, USA). An exponential decay function (base 10) was used to fit the data in each experiment, and the exponent of the function was expressed as a two-degree polynomial function; the best fit was then obtained by iteration ($r^2 > 0.95$).

Data were analyzed using the SPSS v.16.0 software. Interactive effects among Ca^{2+} concentration, temperature, radiation treatments and exposure time on Y, NPQ, photosynthetic carbon fixation (P), calcification rate (C) and C/P were statistically analyzed using a two, three or four-way ANOVA test to establish significance ($p < 0.05$) among the variables. The Student Newman-Keuls (SNK) test with a level of significance set at $p < 0.05$ was used for post-hoc comparisons. The Student's t-test was also used to analyze growth rates and pigments data.

3   Results

3.1   Carbonate chemistry, growth rates, pigments and morphology

The parameters for the carbonate system of the media are presented in Table 1. Total alkalinity (TA) and CO$_3^{2-}$ concentration were significantly different, with higher TA and CO$_3^{2-}$ levels in the HCa medium. All other parameters did not show significant differences between the two media. After 3 days of culturing and prior to the renewal of media, the pH in both treatments increased to <0.07; the other parameters did not show significant differences among the two Ca^{2+} treatments.

During the acclimation period, reduced Ca^{2+} concentration did not significantly affect growth rates, but it significantly decreased ($p < 0.05$) the chl-*a* and carotenoids contents by 26.7 % and 20 %, respectively (Table 2). The SEM images showed no coccolith-covered surface in cells grown at LCa, and furthermore, the coccoliths were partially dissolved and malformed (Fig. 1a). Instead, cells grown at HCa showed entire and strongly calcified coccoliths (Fig. 1b).

Table 1. Parameters of the artificial seawater carbonate system at the ambient (10 mM) and reduced (0.1 mM) levels of Ca^{2+} equilibrated with ambient CO_2 (39.3 Pa). Total alkalinity, pH, salinity, nutrient concentration and temperature were used to derive all other parameters using a CO_2 system analyzing software (CO_2sys). Data are the means $\pm$ SD of 3 measurements. The asterisks denote significant difference between the two Ca^{2+} concentrations.

Ca^{2+} (mM)	pH_{NBS}	TA ($\mu mol\,kg^{-1}$)	pCO_2 (ppmV)	DIC ($\mu mol\,kg^{-1}$)	CO_2 ($\mu mol\,kg^{-1}$)	HCO_3^- ($\mu mol\,kg^{-1}$)	CO_3^{2-} ($\mu mol\,kg^{-1}$)
10	8.20 ± 0.01	$2539 \pm 12^*$	405 ± 6	2238 ± 11	13 ± 0.2	2008 ± 10	$216 \pm 3^*$
0.1	8.20 ± 0.01	$2496 \pm 24^*$	405 ± 15	2202 ± 28	13 ± 0.5	1979 ± 29	$210 \pm 2^*$

Table 2. Growth rate (in d^{-1}), chl-*a* and carotenoid content (in $pg\,cell^{-1}$) of *Emiliania huxleyi* cells acclimated to 10 mM (HCa) or 0.1 mM Ca^{2+} (LCa) for at least 148 generations. N represents the number of samples. The asterisks represent significant differences between two Ca^{2+} concentrations.

Variable	Ca^{2+} (mM)		p
	10	0.1	
Specific growth rate (d^{-1})	1.07 ± 0.04 ($n = 14$)	1.03 ± 0.05 ($n = 10$)	$p > 0.05$
Chl-*a* ($pg\,cell^{-1}$)	0.15 ± 0.01 ($n = 6$)*	0.11 ± 0.01 ($n = 6$)	$p < 0.001$
Carotenoids ($pg\,cell^{-1}$)	0.30 ± 0.02 ($n = 6$)*	0.24 ± 0.02 ($n = 6$)	$p < 0.01$

3.2 Chl-*a* fluorescence parameters

The main feature of chl-*a* fluorescence parameters was of Y being significantly lower ($p < 0.05$) when samples were exposed to shorter UVR wavebands – i.e., the lowest Y was determined in the 280–700 nm range whereas the highest was in the 400–700 nm (Fig. 2). Additionally, at 20 °C, significantly higher ($p < 0.05$) Y values were determined in the HCa as compared to the LCa treatment. Furthermore, at 20 °C, the Y differences among Ca^{2+} treatments decreased significantly ($p < 0.05$) as the experiment progressed (i.e., at different times of exposure to radiation). After 40 (Fig. 2a) and 80 min (Fig. 2b) of exposure under the solar simulator, Y values at all radiation treatments were significantly higher ($p < 0.05$) in the HCa than in the LCa treatment. However, there were no significant differences ($p = 0.06$) after 2 h (Fig. 2c) of exposure to radiation. There was a significant effect of temperature (as seen in the ratio of Y at the two tested temperatures) with samples in the LCa treatments having significantly higher ($p < 0.05$) Y values at 25 °C than at 20 °C when incubated during 40 (Fig. 2a) and 80 min (Fig. 2b), while there were no differences after 2 h of incubation (Fig. 2c). In contrast, samples in the HCa treatment had always significantly higher ($p < 0.05$) Y values at 20 °C as compared to those at 25 °C, resulting in $Y_{25/20}$ ratio <1 at all incubation times.

The inhibition of Y due to UVA, UVB and UVR at different incubation times is shown in Fig. 3. In general, the Y inhibition increased with increasing exposure time to UVR

wavebands. HCa had significantly but slightly lower inhibition ($p < 0.05$) than LCa treatments at 40 min and 80 min, but there were no significant differences between the two Ca^{2+} concentrations after 2 h. However, inhibition of Y due to UVA (Fig. 3a) decreased slightly but significantly with time ($p < 0.001$), whereas that due to UVB slightly increased ($p < 0.001$). For UVA-induced inhibition (Fig. 3a) values of $\sim$21–34 % were determined after 40 min of exposure whereas they were slightly lower after 80 min ($\sim$13–20 %) and 2 h ($\sim$10–16 %). UVB-induced inhibition of Y was higher (i.e., >40 %) than that due to UVA and increased with exposure time from values of $\sim$41–50 % at 40 min to $\sim$55–60 % after 2 h of exposure (Fig. 3b). The UVR-induced inhibition of Y (Fig. 3c) varied from $\sim$71–77 % and $\sim$62–74 % for LCa and HCa, respectively.

Figure 4 shows the responses of one photoprotective mechanism, as assessed through thermal dissipation of excess energy (i.e., non-photochemical quenching, NPQ). The general pattern was of higher NPQ values ($p < 0.05$) with increasing exposure to UVR wavebands, so that those samples receiving UVR wavelengths had higher NPQ than those receiving only PAR. Additionally, for any radiation treatment, there was a trend for higher NPQ values ($p < 0.05$) at high temperatures, which was especially evident in incubations lasting 80 min (Fig. 4b). Another interesting feature was of higher NPQ values ($p < 0.05$) in HCa than in LCa cells for any radiation treatment at 20 °C; again, this trend was more evident during short time exposures (Fig. 4a) than at the end of the incubation (i.e., after 2 h, Fig. 4c). With
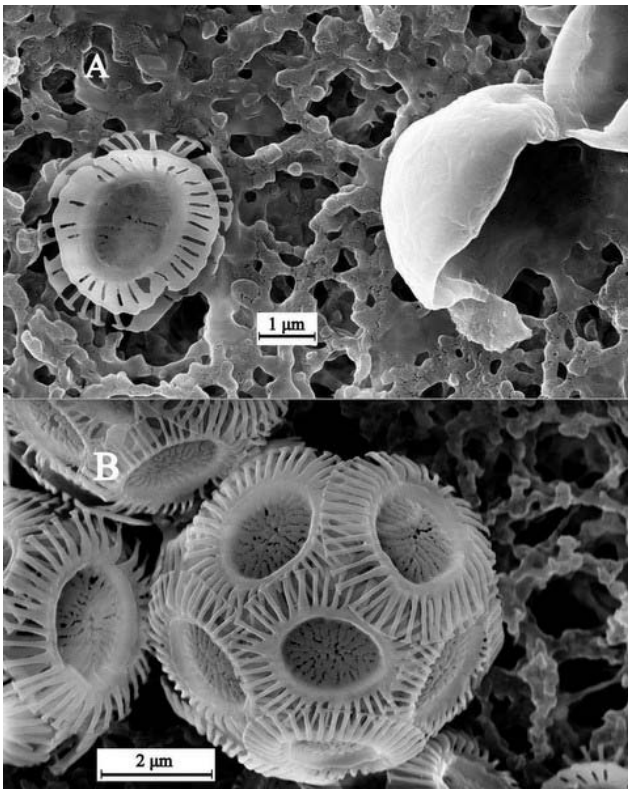
Fig. 1. Scanning electron microscope images of *Emiliania huxleyi* cells grown at: **(A)** 0.1 mM Ca^{2+} and, **(B)** 10 mM Ca^{2+} grown at 20 °C and under PAR illumination of 150 μmol m^{-2} s^{-1}.

increasing exposure time, NPQ at 25 °C of HCa cells decreased ($p < 0.05$) whereas in LCa increased ($p < 0.05$), so that NPQ differences between the two temperature levels decreased in the HCa-grown cells and increased in the LCa-grown ones, respectively. After 2 h, there was no significant difference between the two Ca^{2+} concentrations at 20 °C ($p > 0.05$, Fig. 4c).

3.3 Photosynthetic carbon fixation (P), calcification rates (C) and C/P

Photosynthetic carbon fixation of *Emiliania huxleyi* (Fig. 5a) was stimulated by eliminating the shorter wavelengths of the spectrum. The general pattern was of higher photosynthetic carbon values ($p < 0.05$) in the HCa-grown than in the LCa-grown cells. The beneficial effect of temperature was clearly evident in samples acclimated to HCa (Fig. 5a) so that, for example, the highest photosynthetic carbon at 25 °C (Fig. 5a) was 0.76 pg C cell^{-1} h^{-1} whereas at 20 °C was 0.58 pg C cell^{-1} h^{-1}. Under PAR alone (i.e., >395 nm treatment), however, high temperature significantly inhibited photosynthesis ($p < 0.05$) by 10.1 % in the LCa-grown cells. Under UVR, high temperature did not show significant effects on carbon incorporation in the LCa-grown cells.
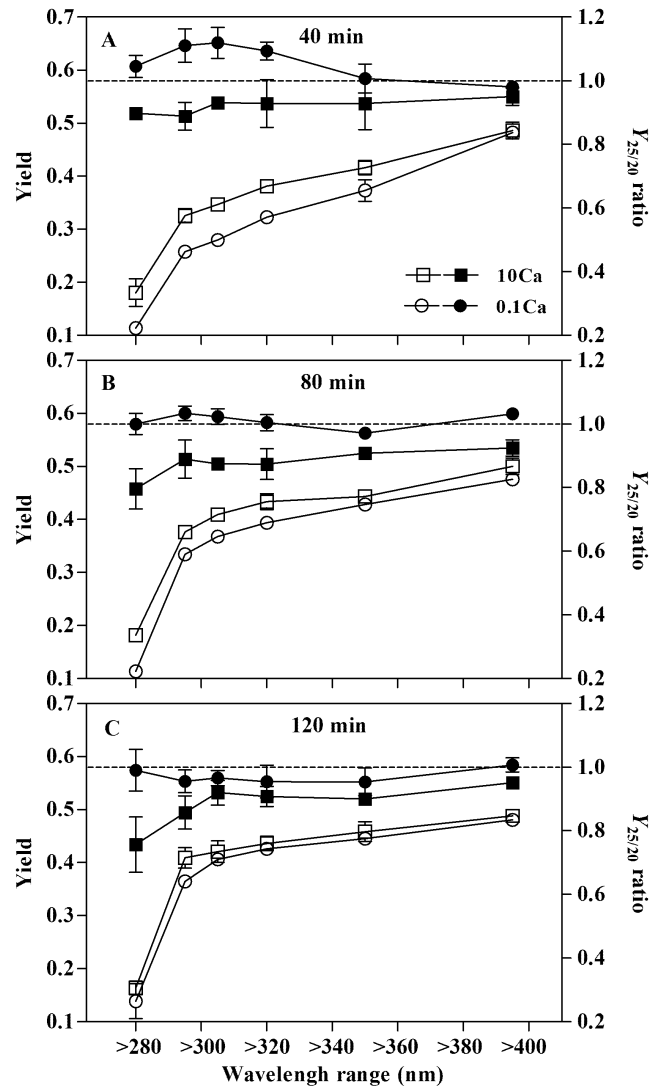

Fig. 2. Effective photochemical quantum yield (F'_v/F'_m) of *Emiliania huxleyi* cells grown at HCa (squares) and LCa (circles). Open symbols indicate F'_v/F'_m measured at 20 °C whereas black symbols indicate the ratio of F'_v/F'_m measured at 25 °C to that at 20 °C. Measurements done after exposures to artificial radiation: **(A)** 40 min, **(B)** 80 min and, **(C)** 120 min. The bars on top of the symbols represent the standard deviation ($n = 3$).

Similar responses were determined in regard to calcification rates (Fig. 5b) with the highest values determined under PAR alone, further benefited by high temperatures especially in the HCa-grown cells, in which calcification rates increased from 0.21 to 0.30 pg C cell^{-1} h^{-1} at 20 and 25 °C, respectively. Calcification rates of LCa were low for all radiation and temperatures treatments. The calcification to photosynthesis ratio (C/P) of the HCa-grown cells increased slightly with increasing wavelength (Fig. 5c) but there was no clear effect of temperature at both Ca^{2+} concentrations.
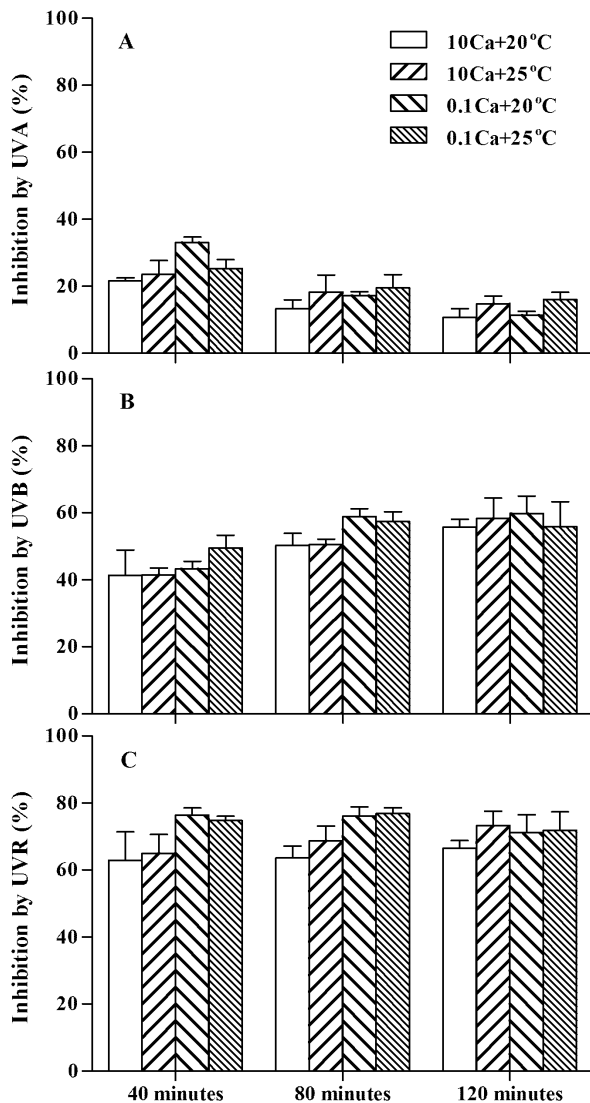
Fig. 3. Inhibition of the effective photochemical quantum yield of *Emiliania huxleyi* cells due to: **(A)** UVA, **(B)** UVB and, **(C)** UVR after 40, 80 and 120 min of exposure to artificial radiation. The lines on top of the bars represent the standard deviations ($n = 3$).

Fig. 4. Non photochemical quenching (NPQ) of *Emiliania huxleyi* cells grown at HCa (squares) and LCa (circles) and exposed to different radiation and temperature treatments. Open and filled symbols are cells exposed at 20 °C and 25 °C, respectively. Measurements done after exposures to artificial radiation: **(A)** 40 min, **(B)** 80 min and, **(C)** 120 min. The bars on top of the symbols represent the standard deviation ($n = 3$).

Figure 6 shows the relative contribution of UVA and UVB in causing inhibition of photosynthesis, calcification and C/P. For photosynthesis and calcification, higher inhibition ($p < 0.05$) by UVB as compared to that of UVA was determined. For both Ca^{2+} treatments, however, temperature did not show significant effects on inhibition of photosynthetic carbon fixation and calcification rates ($p > 0.05$, Fig. 6a and b). Finally, UVA induced inhibition of C/P showed significant ($p < 0.05$) differences among the two Ca^{2+} concentrations (Fig. 6c), but it did not among temperatures. Shorter wavelengths of UVB showed opposite responses: UVB-induced inhibition of C/P was significantly different among the two Ca concentrations, being positive for
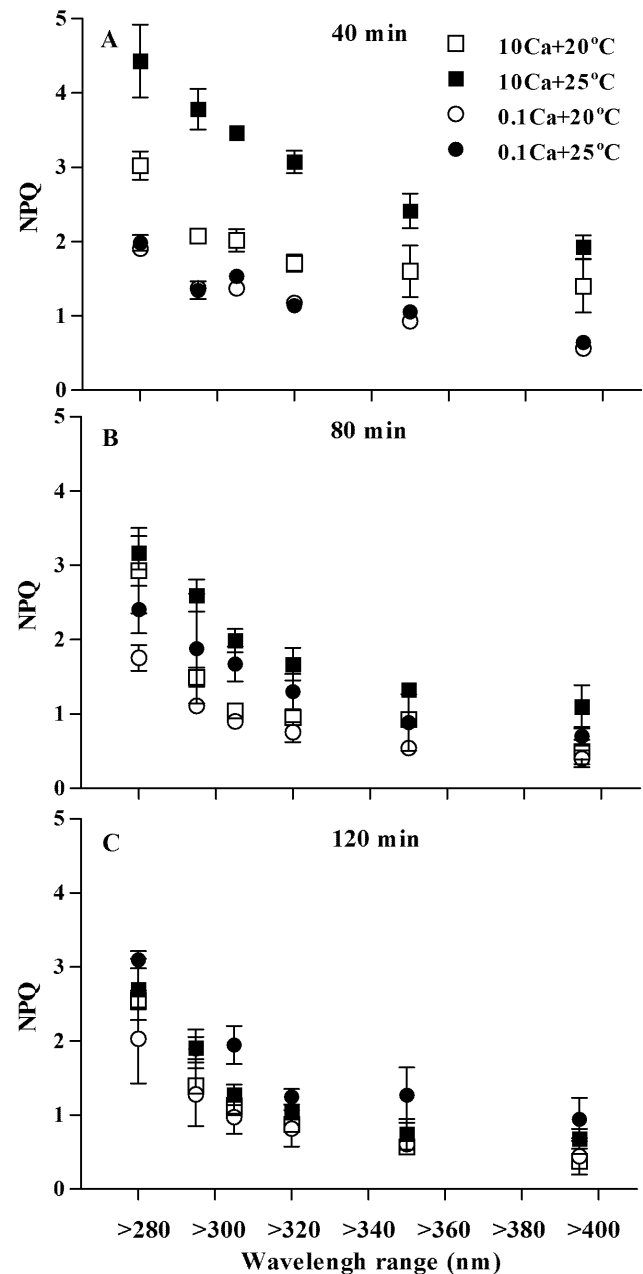
the HCa-grown and negative for the LCa-grown cells, respectively (Fig. 6c). Furthermore, high temperature significantly reduced inhibition of C/P due to UVB ($p < 0.001$, Fig. 6c).
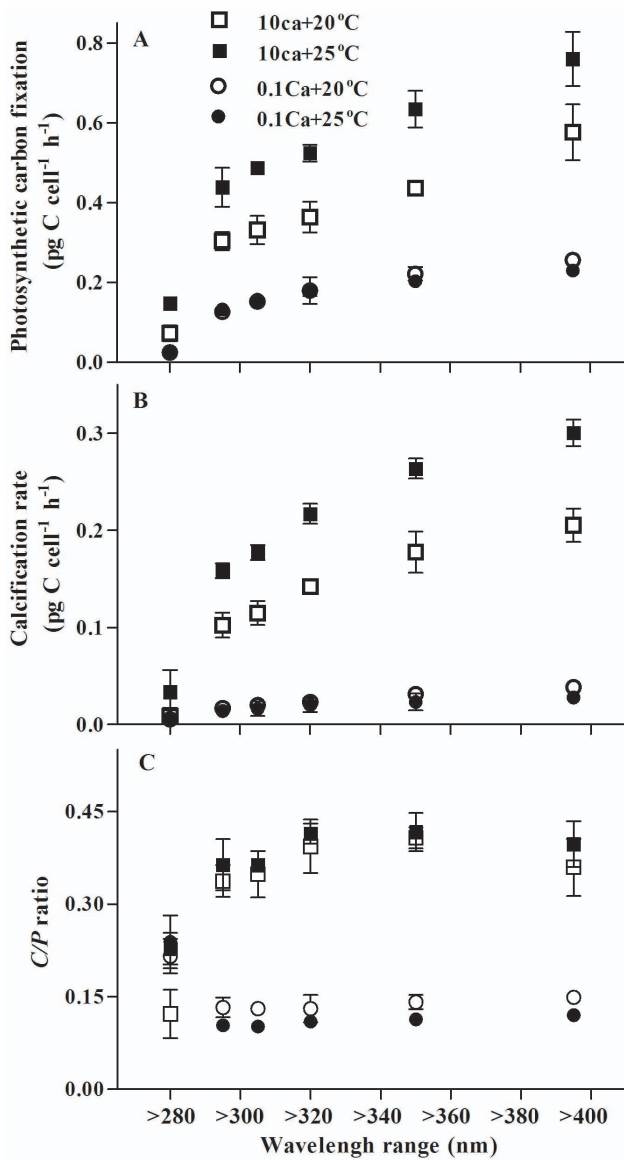
Fig. 5. **(A)** Photosynthetic carbon fixation (in $pg\,C\,cell^{-1}\,h^{-1}$), **(B)** Calcification rate (in $pg\,C\,cell^{-1}\,h^{-1}$) and, **(C)** *C/P* ratio of *Emiliania huxleyi* cells grown at HCa (squares) and LCa (circles) and exposed to different radiation and temperature treatments for 2 h. Open and filled symbols are cells exposed at 20 °C and 25 °C, respectively. The bars on top of the symbols represent the standard deviation ($n = 3$).

3.4 BWF

There were similar trends of BWFs for inhibition of *Y* (Fig. 7a), photosynthetic carbon fixation (Fig. 7c) and calcification (Fig. 7d) with decreasing weights towards higher wavelengths. On the other hand, BWFs for inhibition of NPQ (Fig. 7b) showed an opposite response i.e., NPQ was promoted by exposure to short wavelengths. In general, all BWFs did not exhibit significant differences among the two Ca concentrations and the two temperatures tested.
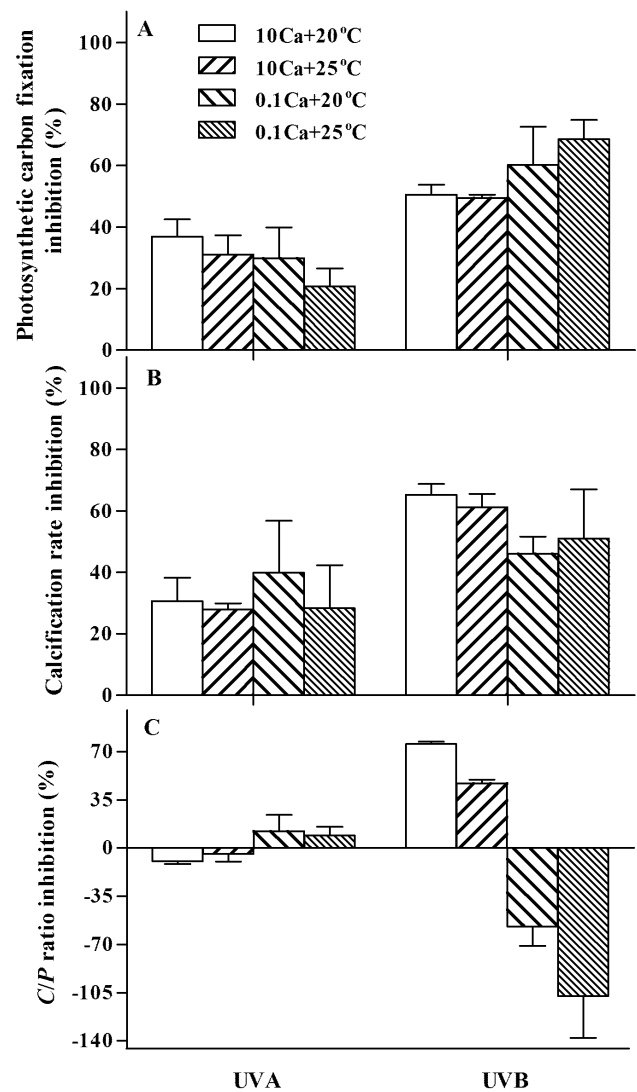

Fig. 6. UVR-induced inhibition of **(A)** Photosynthetic carbon fixation, **(B)** Calcification rate and, **(C)** *C/P* ratio of *Emiliania huxleyi* cells. The lines on top of the bars represent the standard deviations ($n = 3$).

4 Discussion

The results of our study can be summarized as follows: (1) decreased calcification resulted in a decrease of photoprotective mechanisms (NPQ), pigments contents and photosynthetic carbon fixation; (2) calcification and photosynthesis (and their ratio) showed different responses related to UVR, with the HCa-grown cells having more tolerance to UVR than the LCa-grown ones; (3) elevated temperature increased photosynthesis and calcification of *Emiliania huxleyi*, grown at high Ca^{2+} concentrations whereas the opposite was observed in low Ca^{2+} grown cells. In the following paragraphs we will discuss the possible causes of the differential responses observed in our study.
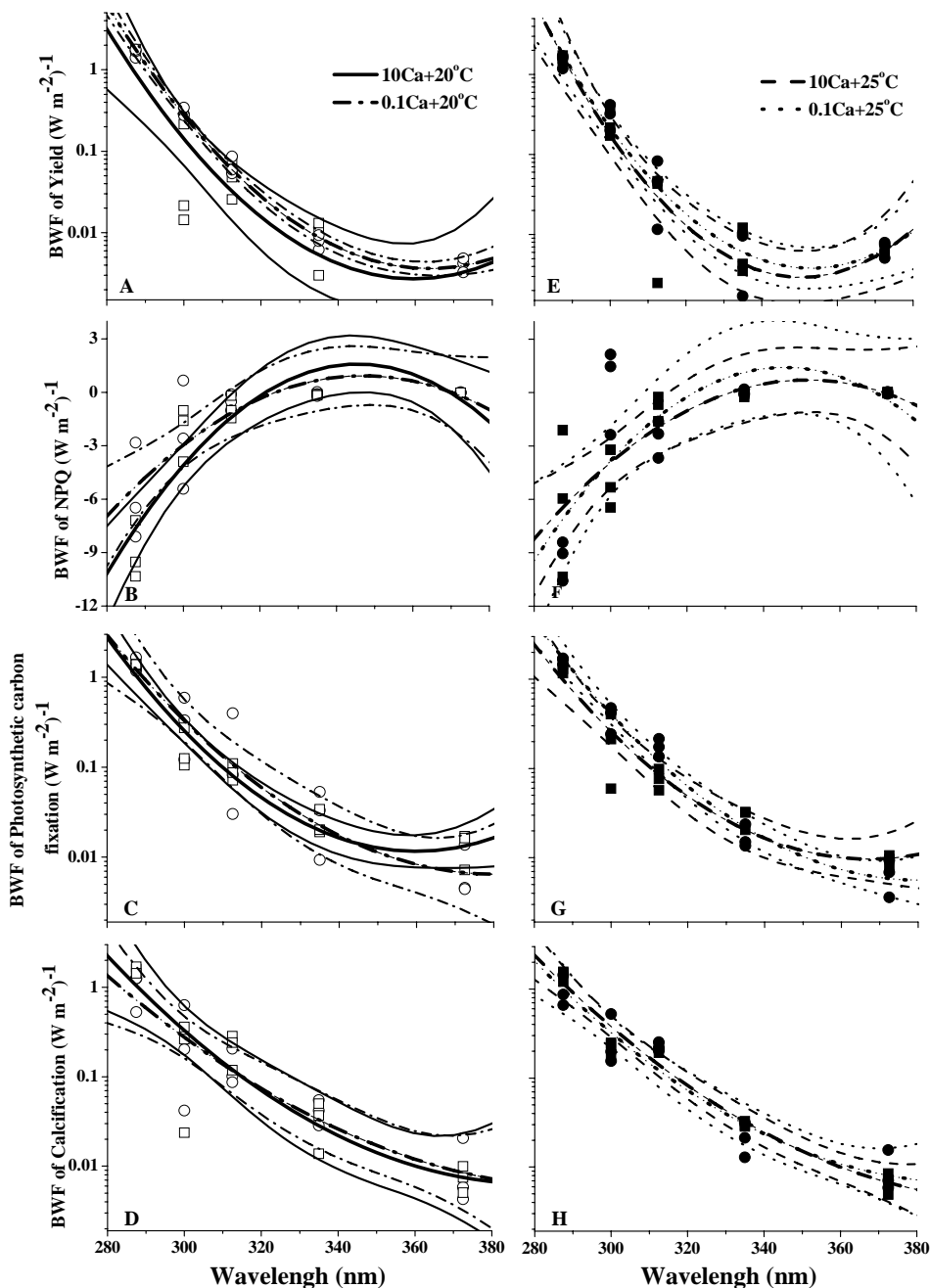
Fig. 7. Biological weighting functions (BWFs, in $(W\,m^{-2})^{-1}$) of *Emiliania huxleyi*: (**A** and **E**) effective photochemical quantum yield (Y); (**B** and **F**) non photochemical quenching (NPQ); (**C** and **G**) photosynthetic carbon fixation and, (**D** and **H**) calcification rate of cells grown at HCa and LCa concentrations. The symbols represent the different combinations of Ca^{2+} concentration and temperature: open squares: HCa cells at 20 °C; filled squares: HCa cells at 25 °C; open circles: LCa cells at 20 °C and filled circles: LCa cells at 25 °C.

Emiliania huxleyi depends on Ca^{2+} to form carbonate crystals that build up the coccolith shell that shelters the cells. Ca^{2+} availability is also associated to other process, as seen in other studies (Trimborn et al., 2007; Leonardos et al., 2009) that demonstrated that cells grown under low (0.1 mM Ca^{2+}) or without Ca^{2+} decreased their growth rates

as compared to those cultured under higher Ca^{2+} concentrations (e.g., 1–10 mM). Similarly, in our study we determined a significant decrease in the growth rates of *E. huxleyi* cells after being transferred from 10 mM Ca^{2+} to 0.1 mM Ca^{2+}, but only during the initial 12 generations in 9 days (data not shown). After 100 days (148 generations), there were no

significant differences in growth rates between the two Ca^{2+} concentrations (Table 2), clearly suggesting that acclimation to the lowered Ca^{2+} level took longer time than expected (Herfort et al., 2002, 2004; Trimborn et al., 2007; Leonardos et al., 2009). Nevertheless, significant differences between the two Ca^{2+} concentrations were observed in the amount of pigments – chl-*a* and carotenoids per cell (Table 2). The increased contents of the photosynthetic pigments are probably due to the reduced radiation levels received by HCa-grown cells, which had coccolith shelter. In fact, it was previously shown that the coccolith layer reduces the transmission of both UV and PAR, i.e., over 15 % of PAR was absorbed by the coccolith layer compared to naked cells (Gao et al., 2009); therefore, LCa-grown cells with less or without coccoliths received relatively more radiation. Consequently, after long-term acclimation to less radiation the HCa-grown cells upregulated their contents of chl-*a*, with an increase of the antenna size, reflecting a classical shade adaptation behavior.

The *E. huxleyi* cells grown at the high Ca^{2+} concentration had higher photosynthetic carbon fixation, calcification rate and more tolerance to UVR than those grown at low Ca^{2+} concentration. In addition, under UVR exposure, elevated temperature enhanced photosynthesis of the HCa-grown cells as compared to the LCa-grown ones (Figs. 2 and 5). There are several mechanisms that might account for part of the observed variations in the responses. For example, dissipation of excess energy as heat (NPQ) is a well known photoprotective mechanism occurring in aquatic photoautotrophs (Falkowski and Raven, 1997). UVR can have a fast induction of NPQ by increasing PSII inactivation, reducing RUBISCO activity and enhancing xanthophylls de-epoxidation (Van de Poll et al., 2009). So, NPQ increased as shorter UVR wavelengths were received by the cells (Fig. 4), but at the same time, photosynthetic carbon fixation and *Y* decreased (Figs. 2 and 5). In our case, cells acclimated to HCa had higher NPQ values, at least during short-term incubations, as compared to those under LCa (Fig. 4). Many studies have shown that NPQ and F_v'/F_m' behave as mirror images, with increases in NPQ inversely correlated with decreases in F_v'/F_m' (Adams III. and Demmig-Adams, 2004). Carotenoids involved in the xanthophylls cycle may also play an important role in maintaining the energy balance. This cycle has been shown to contribute to photoprotection under visible light by thermal dissipation of excess excitation energy (Demmig-Adams, 1990). Moreover, while UVR-induced reactive oxygen species (ROS) could damage lipids, DNA and proteins (He and Häder, 2002), carotenoids could scavenge singlet oxygen and other ROS (Bornman et al., 1997) thus allowing cells to reduce or minimize stress. Therefore, it is possible that the higher concentration of carotenoids in the HCa-grown cells might have partially helped them to cope with damaging UVR wavelengths. It is obvious that higher NPQ values coincided with higher calcification rates (Figs. 4 and 5), but overall NPQ values

decreased with time in both Ca^{2+} treatments, and also with exposure to longer wavelength (Fig. 4). This implies that calcification plays a role as an alternative way to protect the cells from excessive energy. It is known that as an energy dependent process, calcification involves the cellular uptake of dissolved inorganic carbon and Ca^{2+} from the extracellular medium into the coccolith vesicle and the production of coccolith polysaccharides (Brownlee and Taylor, 2004).

After acclimation to the low Ca^{2+} concentration, calcification and photosynthesis at 20 °C decreased by 81.3 % and 55.4 % (Fig. 5). Other studies (Herfort et al., 2002, 2004; Trimborn et al., 2007; Leonardos et al., 2009) however, found that low Ca^{2+} concentrations did not affect the POC production, photosynthetic carbon fixation or photosynthetic oxygen evolution. In addition, Trimborn et al. (2007) using SEM analysis found naked cells but not coccoliths or even residues, and they concluded that cells did not calcify at 0.1 mM Ca^{2+} concentrations. In general, it can be considered that calcite dissolution occurs when the calcite saturation state (Ω) is <1 (Trimborn et al., 2007). In our study, and although some part of the coccolith layer dissolved under the calcium carbonate undersaturated conditions (Ω <0.1), our SEM analysis of the LCa-grown cells showed that they did not lose the capacity to produce coccoliths (Fig. 1). In the case of our LCa cells, calcification decreased to 18.7 % as compared to cells grown at ambient Ca^{2+} concentration (HCa, Fig. 5). Therefore, the LCa-grown cells might not need energy as much as the HCa-grown cells do to calcify due to reduced availability of Ca^{2+}. Then photosynthetic activity were down-regulated, as reflected by the lower *Y* and carbon fixation rates. A decrease in calcification rates in *E. huxleyi* is expected to decrease photosynthesis rates having a negative feedback that further reduces calcification. This is well consistent with the fact that no difference in the growth rates was found between the LCa-grown and the HCa-grown cells (Table 2), which reflected the net energy balance.

Cells grown at LCa and HCa displayed significant differences in the inhibition of C/P (Figs. 5, 6 and 7). Moreover, the responses of photosynthesis and calcification towards UVR appear to be not synchronous. In this sense, Paasche (1966) found that calcification and photosynthesis of *Emiliania huxleyi* had different action spectra, as for example blue light appeared to be more efficient in calcification than in photosynthetic carbon fixation. In our study, and in agreement with a previous work (Gao et al., 2009), we showed no UVA impact on the C/P ratio of *E. huxleyi* but a significant UVB-induced decrease of C/P. However, some differences might arise when considering the responses on more dense cultures (Guan and Gao, 2010) with shorter wavelengths of UVB causing more damage to photosynthesis than to calcification, and longer wavelengths of UVA resulting in a decrease of calcification; in general terms, large cell density affects the control of the carbonate system (Gattuso et al., 2010). The irradiance levels of PAR, UVA and UVB used by us in our experiments were respectively about 18.1, 43.6 and

60 % of the maximum values measured in the South China Sea where coccolithophores are abundant (Ho et al., 2010; Li et al., 2011). Previous studies (Guan and Gao, 2010) indicated that *E. huxleyi* response changed with the irradiance and this was the base to use BWFs with an exposure response model based on irradiance (Neale and Kieber, 2000). The "chronic" and/or "dynamic" (i.e., reversible) effects would depend on the irradiance levels and the presence of threshold values above which any effects can be observed (Helbling et al., 1992). In addition, senescent and nutrient-limited cells tend to acquire extra layers of coccoliths (Paasche, 2002; Shiraiwa, 2003). Furthermore, and as previously mentioned, the coccolith layer around the cell surface could effectively reduce the transmission of UVB (Gao et al., 2009). Additionally, for *E. huxleyi* stain CS-369, both lowering Ca^{2+} concentration and elevated CO_2/decreased pH (Gao et al., 2009) led to a decrease in calcification. However, it is still unknown whether these two different ways have common mechanisms on regulation of calcification process.

The observed increase in photosynthesis of HCa cells under high temperature (Fig. 5) was similar to the results obtained by Feng et al. (2008). Photosynthetic carbon fixation is largely controlled by enzymes related to dark reactions (Falkwoski and Raven, 1997) and so its rate should also be temperature-dependent, with the enzymes involved in photosynthetic carbon fixation and calcification being stimulated by high temperatures. Additionally, phosphatase activity in *E. huxleyi* decreased with reduced Ca^{2+} concentrations as shown in a previous study (Shaked et al., 2006). Thus, if the enzymes of *E. huxleyi* were affected by long time acclimation to low Ca^{2+} concentration, this may have contributed to the different response of photosynthesis and calcification between two experimental Ca^{2+} concentrations (Fig. 5). In fact in our study, the calcification of *E. huxleyi* significantly increased at high temperatures (Fig. 5). However, Feng et al. (2008) did not observe such a significant effect of elevated temperature on calcification of this coccolithophore. Moreover, a 5 °C increase in temperature (from 13 to 18 °C) decreased the calcification rate of *E. huxleyi* grown at both, present and future CO_2 concentrations (De Bodt et al., 2010). It is likely that the differential responses of photosynthesis and calcification at different levels of temperature are responsible for such discrepancies, since photosynthetic carbon fixation process could be more sensitive to temperature as compared to calcification in this species. However, it can not be ruled out that specific responses among different strains, or counteracting effects due to differences in pH are also responsible for differences in responses to UVR even within the same species.

The ongoing ocean acidification is compounded with the shoaling of the mixed layer, increased surface seawater temperature and increased exposures of the cells to high radiation levels. Many studies focused on the effects of ocean acidification on coccolithophore (Riebesell et al., 2000; Feng et al., 2008; Iglesias-Rodriguez et al., 2008; De Bodt et al.,

2010), but few considered the role of UVR in natural conditions (Gao et al., 2009). Our results indicate that reduced calcification in *E. huxleyi* made the cells more vulnerable when they are exposed to excessive light energy even without UVR considered, since reduced calcification led to down-regualated photoprotective capability. In addition, increased temperature decreased the C/P ratio in the LCa-grown cells. Combined with the previous finding that reduced calcification led to enhanced sensitivity to UVR and decreased ratio of C/P (Gao et al., 2009), the combined effects of ocean acidification, global warming and increased light and UVR exposures will synergistically reduce the C/P ratio, which would eventually affect the carbon-related biogeochemical processes.

References

Adams III., W. W. and Demmig-Adams, B.: Chlorophyll fluorescence as a tool to monitor plant response to the environment, in: Chlorophyll a Fluorescence: A Signature of Photosynthesis, edited by: Papageorgiou, G. C. and Govindjee, Springer, Berlin, Germany, 583–604, 2004.

Anning, T., Nimer, N., Merrett, M. J., and Brownlee, C.: Costs and benefits of calcification in coccolithophorids, J. Marine Syst., 9, 45–56, 1996.

Beardall, J., Sobrino, C., and Stojkovic, S.: Interactions between the impacts of ultraviolet radiation, elevated CO_2, and nutrient limitation on marine primary producers, Photochem. Photobio. S., 8, 1257–1265, doi:10.1039/b9pp00034h, 2009.

Bornman, J. F., Reuber, S., Cen, Y., and Weissenböck, G.: Ultraviolet radiation as a stress factor and the role of protective pigments, in: Plants and UV-B: Responses to Environmental Change, edited by: Lumsden, P. J., Cambridge University Press, Cambridge, NY, 157–168, 1997.

Brownlee, C. and Taylor, A.: Calcification in coccolithophores: a cellular perspective, in: Coccolithophores: From Molecular Biology to Global Impact, edited by: Thierstein, H. R. and Young, J. R., Springer, Berlin, Germany, 31–49, 2004.

Brownlee, C., Davies, M., Nimer, N., Dong, L., and Merrett, M.: Calcification, photosynthesis and intracellular regulation in *Emiliania huxleyi*, B. Inst. Oceanogr. Monaco, 14, 19–35, 1995.

Buma, A. G. J., Van Oijen, T., Van de Poll, W., Veldhuis, M. J. W., and Gieskes, W. W. C.: The sensitivity of *Emiliania huxleyi* (Prymnesiophyceae) to ultraviolet-B radiation, J. Phycol., 36, 296–303, 2000.

Cokacar, T., Kubilay, N., and Oguz, T.: Structure of *Emiliania huxleyi* blooms in the Black Sea surface waters as detected by SeaWIFS imagery, Geophys. Res. Lett., 28, 4607–4610, 2001.

De Bodt, C., Van Oostende, N., Harlay, J., Sabbe, K., and Chou, L.: Individual and interacting effects of pCO_2 and temperature on *Emiliania huxleyi* calcification: study of the calcite production, the coccolith morphology and the coccosphere size, Biogeosciences, 7, 1401–1412, doi:10.5194/bg-7-1401-2010, 2010.

Demmig-Adams, B.: Carotenoids and photoprotection in plants: a role for the xanthophylls zeaxanthin, Biochim. Biophys. Acta, 1020, 1–24, 1990.

Dickson, A. G. and Millero, F. J.: A comparison of the equilibrium constants for the dissociation of carbonic acid in seawater media, Deep-Sea Res., 34, 1733–1743, 1987.

Falkowski, P. G. and Raven, J. A.: Aquatic Photosynthesis, Blackwell Scientific, Oxford, UK, 1997.

Feng, Y., Warner, M. E., Zhang, Y., Sun, J., Fu, F., Rose, J. M., and Hutchins, D. A.: Interactive effects of increased pCO_2, temperature and irradiance on the marine coccolithophore *Emiliania huxleyi* (Prymnesiophyceae), Eur. J. Phycol., 43, 87–98, 2008.

Gao, K., Ruan, Z., Villafañe, V. E., Gattuso, J. P., and Helbling, E. W.: Ocean acidification exacerbates the effect of UV radiation on the calcifying phytoplankter *Emiliania huxleyi*, Limnol. Oceanogr., 54, 1855–1862, 2009.

Genty, B. E., Briantais, J. M., and Baker, N. R.: Relative quantum efficiencies of the two photosystems of leaves in photorespiratory and non-photorespiratory conditions, Plant Physiol. Bioch., 28, 1–10, 1989.

Guan, W. and Gao, K.: Impacts of UV radiation on photosynthesis and growth of the coccolithophore *Emiliania huxleyi* (Haptophyceae), Environ. Exp. Bot., 67, 502–508, 2010.

Gattuso, J. P., Gao, K., Lee, K., Rost, B., and Schulz, K. G.: Approaches and tools to manipulate the carbonate chemistry, in: Guide to best practices for ocean acidification research and data reporting, edited by: Riebesell, U., Fabry, V. J., Hansson, L., and Gattuso, J.-P., Publications office of the European Union, Luxembourg, 41–52, 2010.

Häder, D. P., Helbling, E. W., Williamson, C. E., and Worrest, R. C.: Effects of UV radiation on aquatic ecosystems and interactions with climate change, Photochem. Photobiol. Sci., 10, 242–260, 2011.

He, Y. and Häder, D. P.: Reactive oxygen species and UV-B: effects on cyanobacteria, Photochem. Photobio. S., 1, 729–736, 2002.

Helbling, E. W., Villafañe, V. E., Ferrario, M. E., and Holm-Hansen, O.: Impact of natural ultraviolet radiation on rates of photosynthesis and on specific marine phytoplankton species, Mar. Ecol.-Prog. Ser., 80, 89–100, 1992.

Herfort, L., Thake, B., and Roberts, R. J.: Acquisition and use of bicarbonate by *Emiliania huxleyi*, New Phytol., 156, 427–436, 2002.

Herfort, L., Loste, E., Meldrum, F., and Thake, B.: Structural and physiological effects of calcium and magnesium in *Emiliania huxleyi* (Lohmann) Hay and Mohler, J. Struct. Biol., 148, 307–314, 2004.

Ho, T. Y., Chou, W. C., Wei, C. L., Lin, F. J., Wong, G. T. F., and Lin, H. L.: Trace metal cycling in the surface water of the South China Sea: vertical fluxes, composition, and sources, Limnol. Oceanogr., 55, 1807–1820, 2010.

Iglesias-Rodriguez, M. D., Halloran, P. R., Rickaby, R. E. M., Hall, I. R., Colmenero-Hidalgo, E., Gittins, J. R., Green, D. R. H., Tyrrell, T., Gibbs, S. J., von Dassow, P., Rehm, E., Armbrust, E. V., and Boessenkool, K. P.: Phytoplankton calcification in a high-CO_2 world, Science, 320, 336–340, 2008.

Leonardos, N., Read, B., Thake, B., and Young, J. R.: No mechanistic dependence of photosynthesis on calcification in the coccolithophorid *Emiliania huxleyi* (Haptophyta), J. Phycol., 45, 1046–1051, 2009.

Lewis, E. and Wallace, D. W. R.: Program Developed for CO_2 System Calculations, ORNL/CDIAC-105, Carbon Dioxide Information Analysis Center, Oak Ridge National Laboratory, US Department of Energy, Oak Ridge, Tennessee, 1998.

Li, G., Gao, K., and Gao, G.: Differential impacts of solar UV radiation on photosynthetic carbon fixation from the coastal to offshore surface waters in South China Sea, Photochem. Photobiol., 87, 329–334, 2011.

Mehrbach, C., Culberson, C. H., Hawley, J. E., and Pytkowicz, R. N.: Measurement of the appearent dissociation constants of carbonic acid in seawater at atmospheric pressure, Limnol. Oceanogr., 18, 897–907, 1973.

Mikaelyan, A. S., Pautova, L. A., Pogosyan, S. I., and Sukhanova, I. N.: Summer bloom of coccolithophorids in the northeastern Black Sea, Oceanology, 45 (Suppl. 1), S127–S138, 2005.

Milliman, J. D.: Production and accumulation of calcium carbonate in the ocean: Budget of a nonsteady state, Global Biogeochem. Cy., 7, 927–957, 1993.

Neale, P. J. and Kieber, D. J.: Assessing biological and chemical effects of UV in the marine environment: spectral weighting functions, in: Causes and Environmental Implications of Increased UV-B Radiation, edited by: Hester, R. E. and Harrison, R. M., The Royal Society of Chemistry, Cambridge, 61–83, 2000.

Nanninga, H. J. and Tyrrell, T.: Importance of light for the formation of algal blooms by *Emiliania huxleyi*, Mar. Ecol.-Progr. Ser., 136, 195–203, 1996.

Nimer, N. A., Merrett, M. J., and Brownlee, C.: Inorganic carbon transport in relation to culture age and inorganic carbon concentration in a high calcifying strain of *Emiliania huxleyi*, J. Phycol., 32, 813–818, 1996.

Paasche, E.: Action spectrum of coccolith formation, Physiol. Plant., 19, 770–779, 1966.

Paasche, E.: A review of the coccolithophorid *Emiliania huxleyi* (Prymnesiophyceae), with particular reference to growth, coccolith formation, and calcification photosynthesis interactions, Phycologia, 40, 503–529, 2002.

Pitsyk, G. K.: O kachestvennom sostave fytoplanktona Azovkogo moray (On the qualitiative compostion of phytoplankton in the Sea of Azov), Sevastopol' Biol. Sta. Trudy, 16, 71–89, 1963.

Porra, R. J.: The chequered history of the development and use of simultaneous equations for the accurate determination of chlorophylls a and b, Photosynth. Res., 73, 149–156, 2002.

Price, N. M., Harrison, G. I., Hering, J. G., Hudson, R. J., Nirel, P. M. V., Palenik, B., and Morel, F. M. M.: Preparation and chemistry of the artificial algal culture medium Aquil, Biol. Oceanogr., 6, 443–461, 1988/89.

Riebesell, U., Zondervan, I., Rost, B., Tortell, P. D., Zeebe, R. E., and Morel, F. M. M.: Reduced calcification of marine plankton in response to increased atmospheric CO_2, Nature, 407, 364–367, 2000.

Rost, B. and Riebesell, U.: Coccolithophores and the biological

pump: responses to environmental changes, in: Coccol-
ithophores: From Molecular Biology to Global Impact, edited
by: Thierstein, H. R. and Young, J. R., Springer, Berlin, Ger-
many, 76–99, 2004.

Shaked, Y., Xu, Y., Leblanc, K., and Morel, F. M. M.: Zinc
availability and alkaline phosphatase activity in *Emiliania hux-
leyi*: implications for Zn-P co-limitation in the ocean, Limnol.
Oceanogr., 51, 299–309, 2006.

Shiraiwa, Y.: Physiological regulation of carbon fixation in the
photosynthesis and calcification of coccolithophorids, Comp.
Biochem. Phys. B., 136, 775–783, 2003.

Sikes, C. S. and Wilbur, K. M.: Function of coccolith formation,
Limnol. Oceanogr., 27, 18–26, 1982.

Sikes, C. S., Roer, R. D., and Wilbur, K. M.: Photosynthesis and
coccolith formation: inorganic carbon sources and net inorganic
reaction of deposition, Limnol. Oceanogr., 25, 248–261, 1980.

Strickland, J. D. H. and Parsons, T. R.: A practical handbook of
seawater analysis, B. Fish. Res. Board Can., 167, 49–80, 1972.

Trimborn, S., Langer, G., and Rost, B.: Effect of varying calcium
concentrations and light intensities on calcification and photo-
synthesis in *Emiliania huxleyi*, Limnol. Oceanogr., 52, 2285–
2293, 2007.

Van de Poll, H. W. and Buma, A. G. J.: Does ultraviolet radiation af-
fect the xanthophyll cycle in marine phytoplankton?, Photochem.
Photobio. S., 8, 1295–1301, 2009.

Villafañe, V. E., Sundbäck, K., Figueroa, F. L., and Helbling, E. W.:
Photosynthesis in the aquatic environment as affected by UVR,
in: UV Effects in Aquatic Organisms and Ecosystems, edited
by: Helbling, E. W. and Zagarese, H. E., The Royal Society of
Chemistry, Cambridge, 357–397, 2003.

Zondervan, I.: The effects of light, macronutrients, trace metals and
CO_2 on the production of calcium carbonate and organic carbon
in coccolithophores – A review, Deep-Sea Res. Pt. II, 54, 521–
537, 2007.